

AD-A225 786

TECHNICAL REPORT TR-RD-SS-90-4

THE RELEVANCE OF THE DE BROGLIE RELATION TO
THE HUGONOT ELASTIC LIMIT (HEL) OF SHOCK
LOADED SOLID MATERIALS

James P. Billingsley
James M. Oliver
Aeroballistics Analysis Branch
Systems Simulation and Development Directorate
Research, Development, and Engineering Center

MARCH 1990

DTIC
JUL 1990
1990 3 1990

60

**U.S. ARMY MISSILE COMMAND***Redstone Arsenal, Alabama* 35898-5000

*Approved for public release;
distribution unlimited*

DISPOSITION INSTRUCTIONS

DESTROY THIS REPORT WHEN IT IS NO LONGER NEEDED. DO NOT RETURN IT TO THE ORIGINATOR.

DISCLAIMER

THE FINDINGS IN THIS REPORT ARE NOT TO BE CONSTRUED AS AN OFFICIAL DEPARTMENT OF THE ARMY POSITION UNLESS SO DESIGNATED BY OTHER AUTHORIZED DOCUMENTS.

TRADE NAMES

USE OF TRADE NAMES OR MANUFACTURER'S IN THIS REPORT DOES NOT CONSTITUTE AN OFFICIAL ENDORSEMENT OR APPROVAL OF THE USE OF SUCH COMMERCIAL HARDWARE OR SOFTWARE.

TECHNICAL REPORT TR-RD-SS-90-4

THE RELEVANCE OF THE DE BROGLIE RELATION TO
THE HUGONIOT ELASTIC LIMIT (HEL) OF SHOCK
LOADED SOLID MATERIALS

James P. Billingsley
James M. Oliver
Aeroballistics Analysis Branch
Systems Simulation and Development Directorate
Research, Development, and Engineering Center

MARCH 1990

Accession For	
NSIC 05001	<input checked="checked" type="checkbox"/>
NSIC 100	<input type="checkbox"/>
Unprocessed	<input type="checkbox"/>
Justification	
By	
Distribution/	
Availability Codes	
Avail and/or	
Dist	Special
A-1	

Approved for public release; distribution unlimited



UNCLASSIFIED

SECURITY CLASSIFICATION OF THIS PAGE

REPORT DOCUMENTATION PAGE				Form Approved OMB No. 0704-0188	
1a. REPORT SECURITY CLASSIFICATION UNCLASSIFIED			1b. RESTRICTIVE MARKINGS		
2a. SECURITY CLASSIFICATION AUTHORITY			3. DISTRIBUTION / AVAILABILITY OF REPORT Approved for public release; distribution is unlimited. 1		
2b. DECLASSIFICATION / DOWNGRADING SCHEDULE					
4. PERFORMING ORGANIZATION REPORT NUMBER(S) TR-RD-SS-90-4			5. MONITORING ORGANIZATION REPORT NUMBER(S)		
6a. NAME OF PERFORMING ORGANIZATION Sys Sim Dev Dir RD&E Center		6b. OFFICE SYMBOL (If applicable) AMSMI-RD-SS-AA	7a. NAME OF MONITORING ORGANIZATION		
6c. ADDRESS (City, State, and ZIP Code) Commander U.S. Army Missile Command Attn: AMSMI-RD-SS Redstone Arsenal, AL. 35898-5252			7b. ADDRESS (City, State, and ZIP Code)		
8a. NAME OF FUNDING / SPONSORING ORGANIZATION		8b. OFFICE SYMBOL (If applicable)	9. PROCUREMENT INSTRUMENT IDENTIFICATION NUMBER		
8c. ADDRESS (City, State, and ZIP Code)			10. SOURCE OF FUNDING NUMBERS		
PROGRAM ELEMENT NO.		PROJECT NO.	TASK NO.	WORK UNIT ACCESSION NO.	
11. TITLE (Include Security Classification) The Relevance of the De Broglie Relation to the Hugoniot Elastic Limit (HEL) of Shock Loaded Solid Materials					
12. PERSONAL AUTHOR(S) Billingsley, James P. and Oliver, James M.					
13a. TYPE OF REPORT Final		13b. TIME COVERED FROM Jul 89 TO Dec 89		14. DATE OF REPORT (Year, Month, Day) 1990 March	
				15. PAGE COUNT 27	
16. SUPPLEMENTARY NOTATION					
17. COSATI CODES			18. SUBJECT TERMS (Continue on reverse if necessary and identify by block number)		
FIELD	GROUP	SUB-GROUP	De Broglie Equation, Particle Velocity, Wave Velocity, Hugoniot Elastic Limit, Iron, TNT, Aluminum Alloys, Elastic-Plastic Shock Waves, 6061, 2024		
19. ABSTRACT (Continue on reverse if necessary and identify by block number)					
<p>Under moderate shock loading (a few kilobars) where Elastic-Plastic Shock Phenomena (EPSP) occur in solid materials, two stress waves are created. The first one is essentially an elastic wave and has become known as the Hugoniot Elastic Limit (HEL). The HEL particle velocity, U_{HEL}, can be closely related to the De Broglie particle momentum wave velocity, $V_1 = h/(2md_1)$, where, h is Planck's constant, m is the mass of an atom, and d_1 is the closest distance between atoms in the structure. Classic EPSP test data for iron, aluminum alloys (2024, 6061), and pressed TNT are compared to computed values of V_1 and $2V_1$. Qualitative remarks with respect to particle stability are made which are based primarily on Fitzgerald's analysis ([17]), Chapter 3.)</p>					
20. DISTRIBUTION / AVAILABILITY OF ABSTRACT <input checked="" type="checkbox"/> UNCLASSIFIED/UNLIMITED <input type="checkbox"/> SAME AS RPT. <input type="checkbox"/> DTIC USERS			21. ABSTRACT SECURITY CLASSIFICATION UNCLASSIFIED		
22a. NAME OF RESPONSIBLE INDIVIDUAL Dr. James P. Billingsley			22b. TELEPHONE (Include Area Code) (205) 876-5210		22c. OFFICE SYMBOL AMSMI-RD-SS-AA

DD Form 1473, JUN 86

Previous editions are obsolete

SECURITY CLASSIFICATION OF THIS PAGE

(If Blank)

UNCLASSIFIED

TABLE OF CONTENTS

	<u>Page</u>
LIST OF ILLUSTRATIONS	iv
I. INTRODUCTION	1
II. THE De BROGLIE PARTICLE VELOCITY, $V_1 = H/(2MD_1)$...	2
III. FITZGERALD'S PARTICLE VELOCITY STABILITY CRITERIA	5
IV. EXPERIMENTAL HEL U_{PHL} DATA AND COMPARISON WITH V_1 MAGNITUDES	6
A. Iron	6
B. Aluminum Alloys	7
1. 2024 Alloy	7
2. 6061-T6 Alloy	7
C. Pressed TNT	13
V. CONCLUSIONS	15
IV. RECOMMENDATIONS	16
REFERENCES	17

LIST OF ILLUSTRATIONS

<u>Figure</u>	<u>Title</u>	<u>Page</u>
1	Elastic and Plastic Wave Front Velocity Versus Particle Velocity for Shocked Iron.	8
2	Elastic Wave Particle Velocity Versus Specimen Thickness for Shocked Iron	9
3	Elastic and Plastic Wave Front Velocity Versus Particle Velocity for Shocked 2024 Aluminum Alloy.	10
4	Elastic and Plastic Wave Front Velocity Versus Particle Velocity for Shocked 6061-T6 Aluminum Alloy.	11
5	Elastic Wave Particle Velocity Versus Specimen Thickness for Shocked 6061-T6 Aluminum Alloy.	12
6	Elastic and Plastic Wave Front Velocity Versus Particle Velocity for Shocked TNT ($\rho_0 = 1.648\text{g/cc}$).	14

I. INTRODUCTION

Many solid materials under moderate shock loading exhibit a two-wave structure where the first one is essentially an elastic wave followed by a slower plastic deformation wave front. References [1] through [10] contain experimental data which illustrate this elastic-plastic-shock phenomena (EPSP). Selected wave and particle velocity results from this classic experimental information for iron, aluminum alloys, and pressed TNT are shown in Figures 1 through 6. Various theoretical aspects of EPSP are described in References [7] through [14].

The elastic wave generated under EPSP conditions is called the Hugoniot Elastic Limit (HEL) to distinguish it from a dynamic elastic limit which could occur from less severe transient load conditions [13]. It is noted in reference [12], page 191, that the HEL condition can produce the same effect as a phase transition. That is, an additional wave is formed.

The main purpose of the present report is to provide evidence that the HEL particle velocity, U_{HEL} , is fundamentally determined (or essentially limited) by the De Broglie momentum velocity-wave length relation which applies for any type of particle motion (Reference [15], page 479; and Reference [16], page 433). Consequently, new insight with respect to the EPSP is provided by the fact that experimentally observed steady state, or stable, values of U_{HEL} compare favorably with the De Broglie velocity, V_1 . V_1 is computed for an unperturbed atomic lattice (see Section II). These comparisons are shown herein for shock loaded iron, aluminum alloys, and TNT, which exhibit EPSP and HEL stress waves.

II. THE De BROGLIE PARTICLE VELOCITY, $V_1 = H/(2MD_1)$

Fitzgerald ([17], Chapters 1 and 3) delineated the importance of the De Broglie momentum wave-length particle velocity, V_1 , with regard to impacted solid material behavior. The De Broglie velocity, V_1 , is:

$$V_1 = \frac{h}{2md_1} = \frac{h}{m\lambda_1} \quad (1)$$

Where:

V_1 = Limiting particle velocity which can occur without permanent lattice distortion (plastic flow); or the limit particle propagation velocity in a stationary lattice.
Units are cm/sec or km/sec

h = Planck's Constant
 $= 6.6262 \cdot 10^{-27} \text{ (gram)(cm}^2\text{)/sec}$

m = Mass of one atom, grams

d_1 = Closest distance between the atoms in a crystal lattice, or the atomic spacing in a slip direction, units are cm or angstroms, \AA , ($1 \text{ \AA} = 10^{-8} \text{ cm}$)

λ_1 = $2 d_1$ = wave length associated with the momentum, mV_1 . It is the shortest wave length possible in an undistorted lattice or stationary lattice, cm or \AA .

Table 1 lists V_1 information for iron, aluminum, and TNT ($\rho_0 = 1.648 \text{ g/cc}$). The values for iron and aluminum are from Reference [17]. V_1 for aluminum was employed for the aluminum alloys (2024 and 6061) since they contain a very high percentage of aluminum. For TNT, an average value of the mass (m_{av}) of an atom and the average distance between atoms (d_{1av}) was computed in the manner outlined in Reference [18]. These average values (m_{av} and d_{1av}) were employed in Eq. (1) to compute V_1 for TNT.

Table 2 lists longitudinal elastic wave velocity, C_L , information for the materials considered in this report. Also shown in Table 2 is the elastic wave pressure, P_{v1} , corresponding to the wave velocity, C_L , and the particle velocity, V_1 . This is given by:

$$P_{v1} = \rho_0 C_L V_1 \quad (2)$$

where ρ_0 is the material density (grams/cc).

TABLE 1. Tabulation of V_1 for Iron, Aluminum, and TNT.

TABULATION OF V_1 FOR IRON, ALUMINUM, AND TNT							
Material	ρ_0	m	d_1	V_1	$2V_1$	$\frac{V_1}{2}$	source
~	g/cc	grams $\times 10^{-23}$	A^0 ($10^{-8}cm$)	km/sec	km/sec	km/sec	~
Iron	7.84	9.27	2.48	0.0144	0.0288	0.0072	[17]
Aluminum	2.70	4.48	2.86	0.0258	0.0516	0.0129	[17]
TNT (pressed)	1.648	1.80	2.22	0.0832	0.1664	0.0416	[18], present

TABLE 2. Tabulation of C_L and P_{V1} .

TABULATION OF C_L AND P_{V1}				
Material	ρ_0	C_L	V_1	P_{V1}
~	g/cc	km/sec	km/sec	kbars
Iron	7.84	6.04 [2]	0.0144	6.82
2024 -T4	2.70	6.41 [7]	0.0258	4.46
6061 -T6	2.70	6.23 [8]	0.0258	4.34
TNT	1.648	2.798 [10]	0.0832	3.84

$$P_{V1} = \rho_0 C_L V_1 = \left(\frac{G}{cc} \right) \left(\frac{cm}{\mu - sec} \right) \left(\frac{cm}{\mu - sec} \right) = MBARS$$

$$P(KBARS) = 10^3 P(MBARS)$$

$$1 KBAR = 14,504.0 PSI$$

III. FITZGERALD'S PARTICLE VELOCITY STABILITY CRITERIA

Fitzgerald, utilizing his concept of reversed lattice motion ([17], Chapter 3) shows that particle velocities from approximately $0.50 V_1$ to $0.75 V_1$ are in an unstable region and can jump to values higher than V_1 . Fitzgerald cites experimental results from Professor Bell and co-workers at Johns Hopkins University which support the analytical prediction.

Particle velocities in the immediate region around V_1 appear to be stable.

In addition, Fitzgerald also showed $2V_1$ was an important unstable velocity where excessive distortion would occur. This analytical result also compared favorably with experimental results obtained by Bell and co-workers for aluminum and copper. These experimental data were acquired from end-to-end cylindrical rod impact via diffraction grating instrumentation.

Professor Bell summarizes his results in Reference [21] and lists three critical or transition particle velocities which were experimentally discovered in pure aluminum. They are listed as follows and compared to V_1 for aluminum (2580 cm/sec from Reference [17])

$$V_{cr1} = 1478 \text{ cm/sec} = 0.573 V_1 \approx 0.6 V_1$$

$$V_{cr2} = 3350 \text{ cm/sec} = 1.298 V_1 \approx 1.3 V_1$$

$$V_{cr3} = 5080 \text{ cm/sec} = 1.969 V_1 \approx 2.0 V_1$$

The comparison is remarkably good, particularly for V_{CR1} and V_{CR3} .

Thus there are three important velocity regions:

1. $0.50 V_1$ to $0.75 V_1$; unstable, may jump to a magnitude greater than V_1 .
2. V_1 vicinity; apparently stable.
3. V_1 to $2V_1$; unstable, particle velocities in this region will approach V_1 under "long term" operating conditions. Ample time is necessary to allow particle momentum sharing with a sufficient number of lattice masses, (see [17], pages 72 to 74). This, by definition, is a relaxation time.

IV. EXPERIMENTAL HEL U_{HEL} DATA AND COMPARISON WITH V_1 MAGNITUDES

A. Iron

References [1] through [6] document experimental investigations of shocked iron. Figure 1 depicts experimental data points for HEL wave velocities as a function of the particle velocity. No actual data points for the plastic wave data are shown. Instead, a recommended [6] linear fit to the plastic wave velocity is illustrated. Only a few data points (with considerable scatter) were available for particle velocities less than 0.06 km/sec and the primary focus of the present study was the elastic wave behavior.

Various investigators found that the HEL for iron depended on the test specimen thickness. Figure 2 illustrates experimental U_{HEL} data as a function of test specimen thickness. A very corroborative data point in Figure 2 was found in Figure 14 of Reference [19]. Reference [19] is an historical review article concerning shock physics investigations performed at Los Alamos National Laboratory. The initial particle velocity (free surface velocity divided by 2) was practically identical to V_1 for this specimen thickness (24.7 mm).

V_1 and $2V_1$ indicators for iron are shown in Figures 1 and 2. The experimental values for U_{HEL} vary from approximately $0.5 V_1$ to $2.4 V_1$. Most of the U_{HEL} magnitudes lie between V_1 and $2V_1$.

As shown in Figure 2, $U_{\text{HEL}} \approx 2V_1$ for the thin specimen and U_{HEL} approaches V_1 for thicker specimen. Thus, the initially overdriven "elastic" wave U_{HEL} is not stable near $2V_1$. It decays or relaxes to a stable value (V_1) provided that the sufficient time (travel distance or specimen thickness) is available. This experimentally observed behavior corroborates remarks made in Section III with respect to the unstable region 3 where $V_1 < U_p < 2V_1$.

See also the initial remarks in Section II of Reference [20] with respect to the asymptotic particle velocity decay exhibited by the data in Figure 2. This reference employs dislocation theory to model the observed phenomena.

An earlier phenomenological model for the relaxation time, τ , is developed in Reference [4]. Reference [4] equations for τ and specimen thickness, L , can be written in terms of V_1 and $2V_1$. This is because 0.0140 and 0.0280 mm/ μ -sec appear as constants in the equations and V_1 and $2V_1$ are equal to 0.0144 and 0.0288 mm/ μ -sec respectively. The significance of the number 0.0140 mm/ μ -sec is that it was the observed steady state particle velocity, which is shown in Figure 2 to be V_1 .

B. Aluminum Alloys

1. 2024 Alloy

Reference [7] documents Fowles' classic experimental and theoretical study of EPSP for both hard and soft 2024 aluminum alloy specimens. Initial and final values of the elastic wave free surface velocities ($2 \cdot U_{\text{PHEL}}$) were tabulated in Reference [7]. These U_{PHEL} data are plotted in Figure 3 which apparently indicates that over-driven transient behavior was exhibited by the "elastic" wave particle velocity data for both hard and soft specimens. However, unlike iron, none of the U_{PHEL} magnitudes exceed $2V_1$. The general relevance of the De Broglie velocity, V_1 , to U_{PHEL} behavior is substantiated by these data for 2024 aluminum alloy. Certainly, the U_{PHEL} magnitudes compare reasonably well with V_1 .

2. 6061-T6 Alloy

Experimental EPSP results for 6061-T6 aluminum alloy are documented in References [8] and [9]. Elastic and plastic wave velocities and corresponding particle velocity information from reference [8] is graphically illustrated in Figure 4. U_{PHEL} data from Reference [9] are plotted versus specimen thickness in Figure 5. This U_{PHEL} information was obtained from the initial step rise of the transient free surface velocity (U_{fs}) data in Figures 4, 5, 6, and 7 of Reference [9]. The initial U_{fs} was carefully scaled from these figures and then U_{PHEL} was computed via the well known relation:

$$U_p = U_{\text{fs}}/2 \quad (3)$$

As illustrated in Figure 4 (Reference [8] data), the particle velocities for elastic waves (with no following plastic wave) do not exceed V_1 by more than approximately twenty percent. This indicates that the limiting particle velocity for a true elastic wave was essentially V_1 . When the loading increased to until EPSP began, the "elastic" wave velocity and particle velocity behaved in an erratic manner. This may be indicative of the instability that could be expected where $V_1 < U_{\text{PHEL}} < 2V_1$.

Compared to iron (Figure 2), U_{PHEL} for 6061-T6 (Figure 5) exhibits very weak dependence on the specimen thickness (or time). The trend is that shown by the data collected from Figure 4 of Reference 9. U_{PHEL} magnitudes vary from about $0.80 V_1$ to $1.30 V_1$. Thus for a rather wide range of specimen thicknesses and input shock pressures (P_{max}), U_{PHEL} was within thirty percent of V_1 . The asymptotic stable value of U_{PHEL} was approximately $0.85 V_1$, or essentially V_1 .

These HEL data for 6061-T6 confirm the importance of V_1 and substantiate the remarks in Section III with respect to particle velocity stability when $V_1 < U_{\text{PHEL}} < 2V_1$.

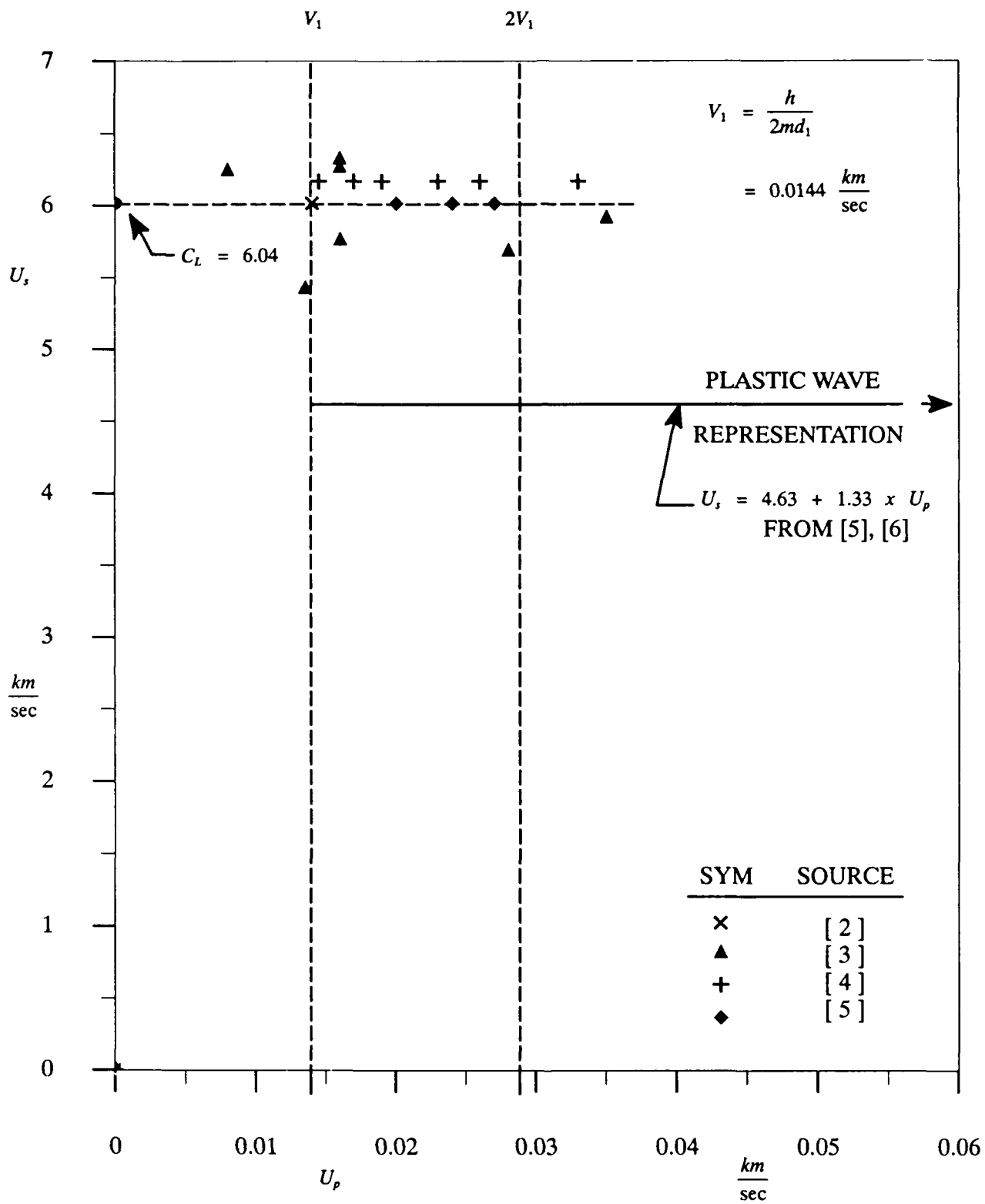


Figure 1. Elastic and Plastic Wave Front Velocity Versus Particle Velocity for Shocked Iron.

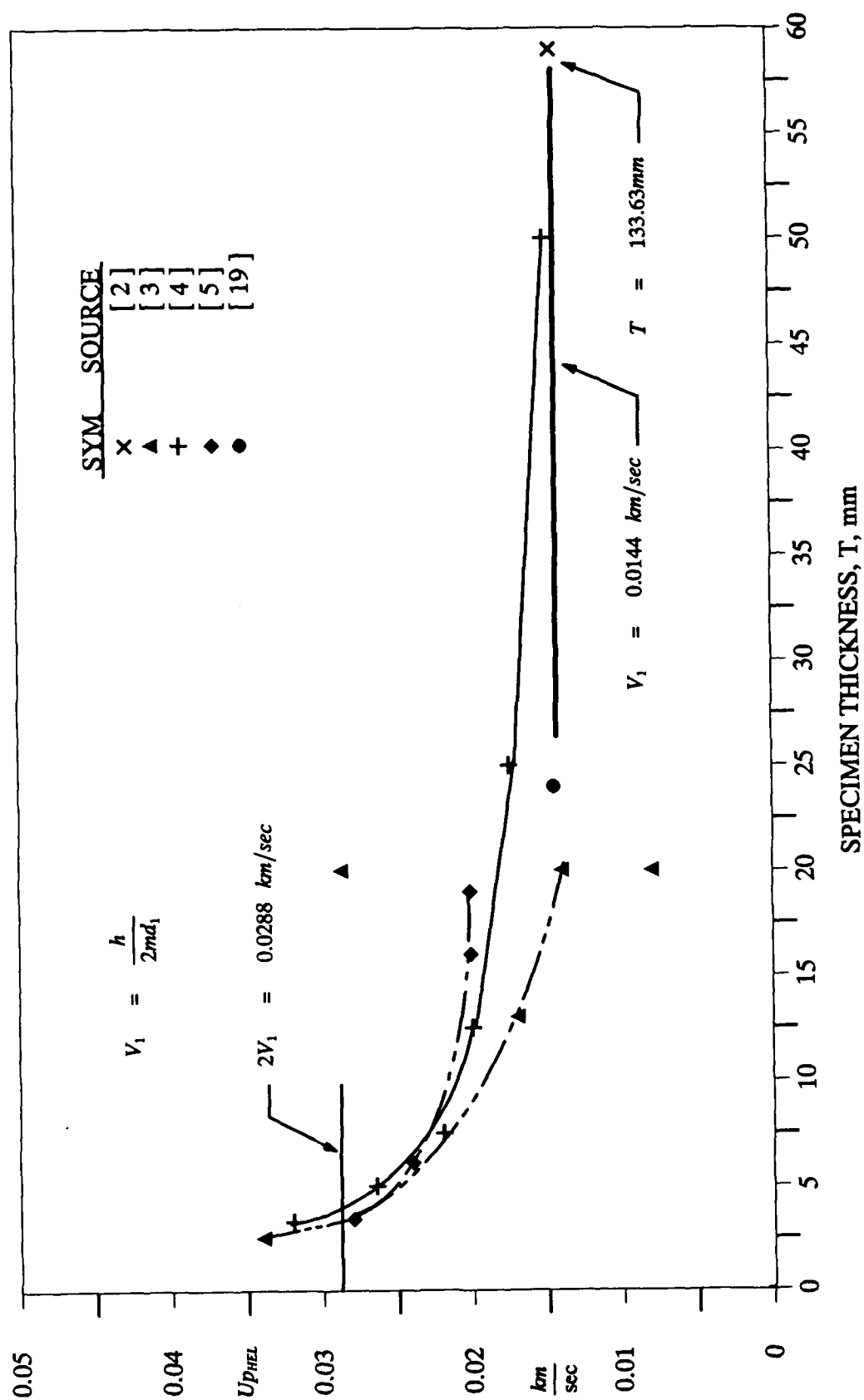


Figure 2. Elastic Wave Particle Velocity Versus Specimen Thickness for Shocked Iron.

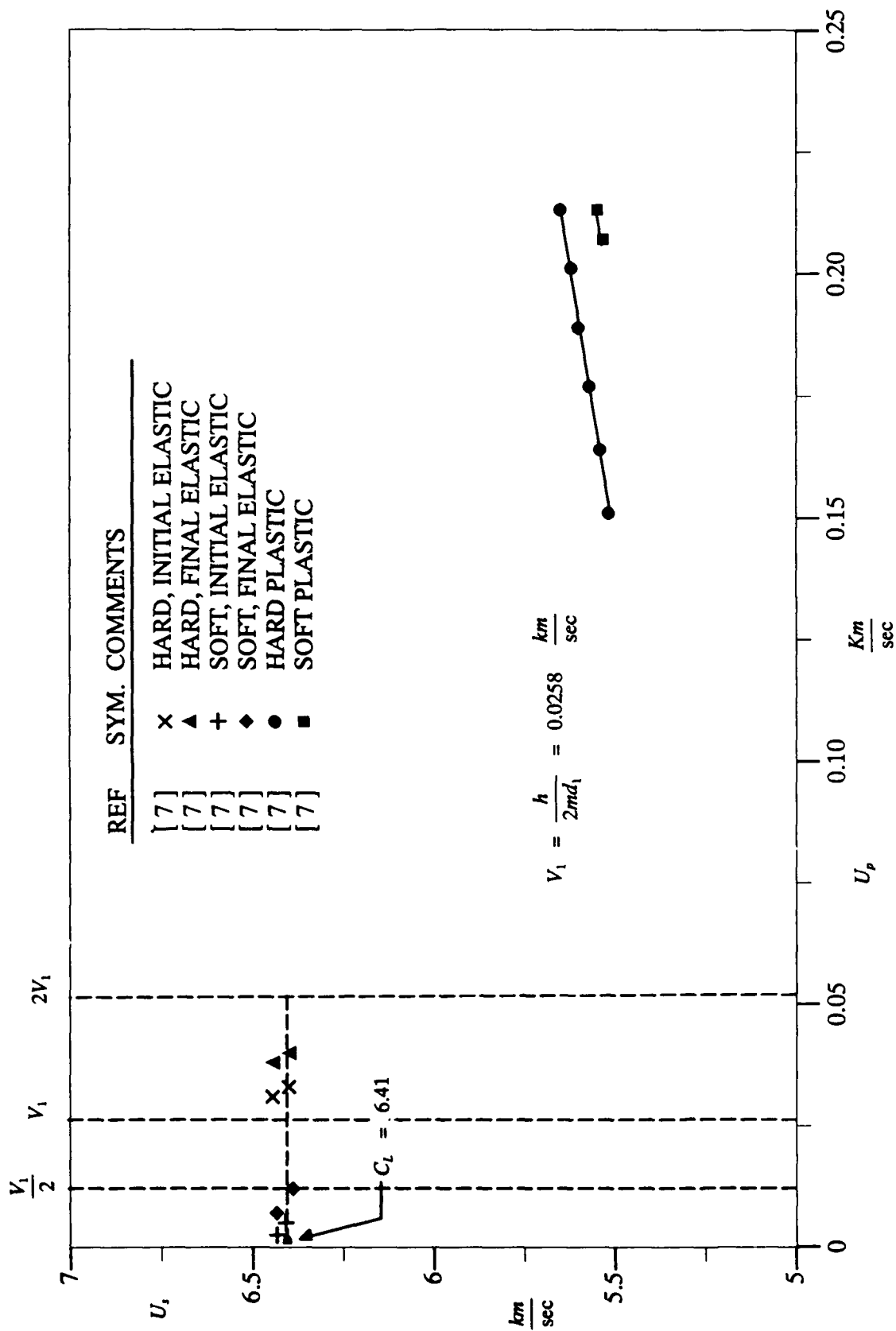


Figure 3. Elastic and Plastic Wave Front Velocity Versus Particle Velocity for Shocked 2024 Aluminum Alloy.

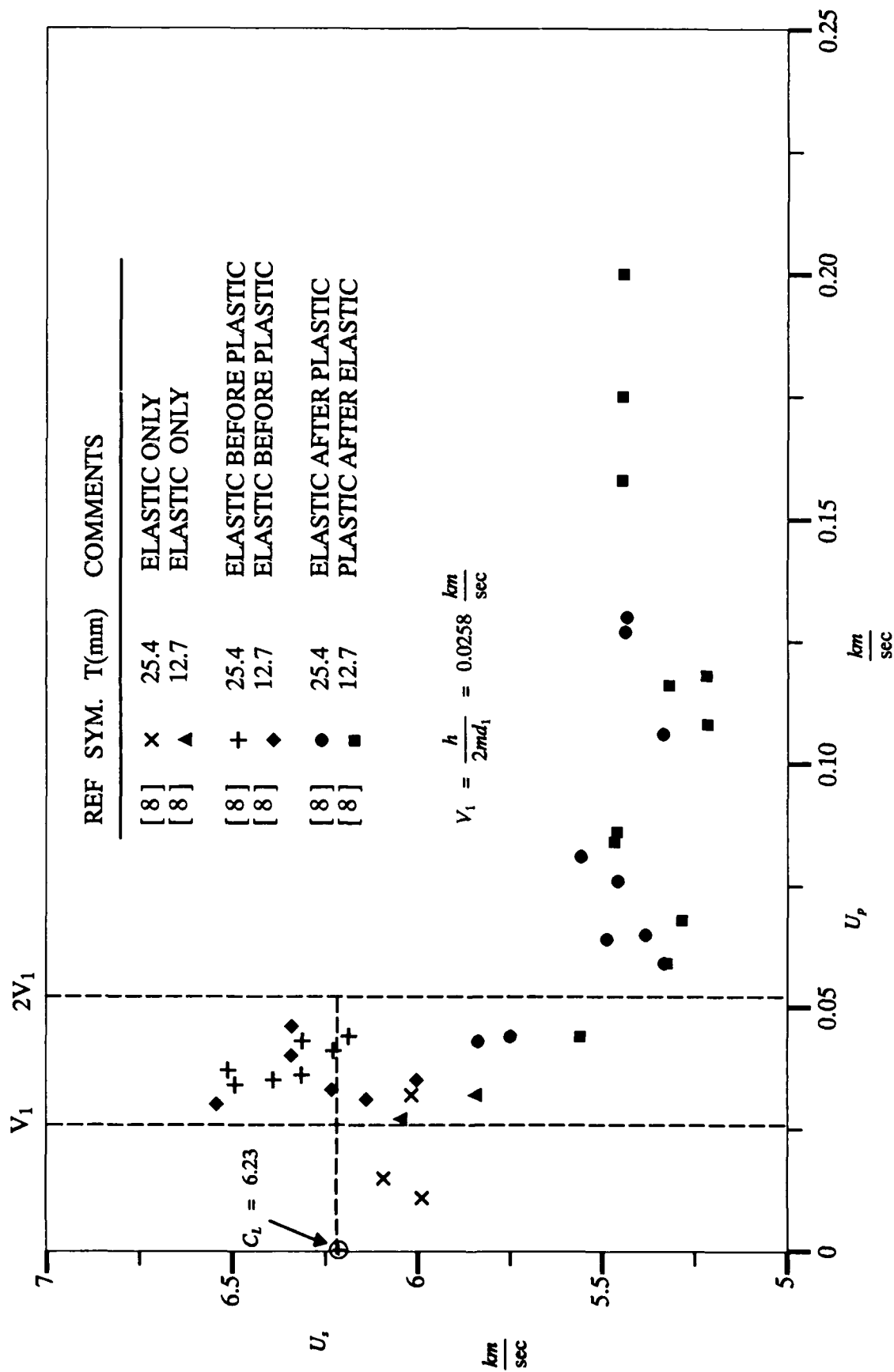


Figure 4. Elastic and Plastic Wave Front Velocity Versus Particle Velocity for Shocked 6061-T6 Aluminum Alloy.

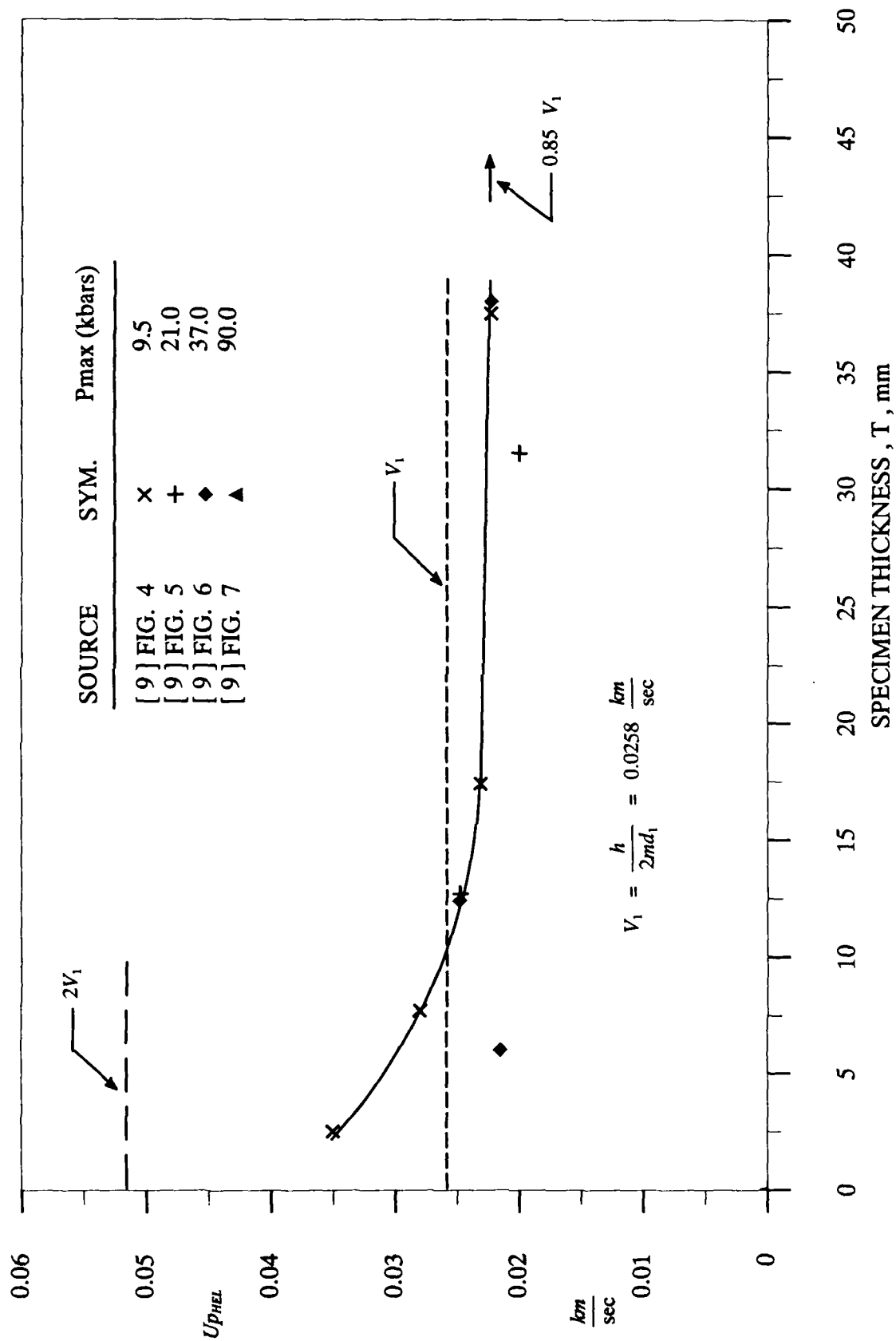


Figure 5. Elastic Wave Particle Velocity Versus Specimen Thickness for Shocked 6061-T6 Aluminum Alloy.

C. Pressed TNT

Very interesting experimental EPSP results for pressed TNT ($\rho_0 = 1.648 \text{ g/cc}$) are reported in Reference [10]. Elastic and plastic wave velocities are plotted as a function of their associated particle velocities in Figure 6. This figure is similar to Figure 6 of Reference [10] and Figure II-13 of Reference [11]. These EPSP data for this polycrystalline organic material exhibit metallic like behavior (see Figures 1, 3, and 4).

Only the V_1 indicator line is drawn in Figure 6 which depicts the pressed TNT EPSP wave and particle velocity experimental results from Reference [10]. Even though there is a specimen thickness size effect on both the HEL wave and particle velocities, none of the HEL particle velocities exceeded V_1 . The highest value of U_{HEL} was 0.0739 km/sec or 0.89 V_1 .

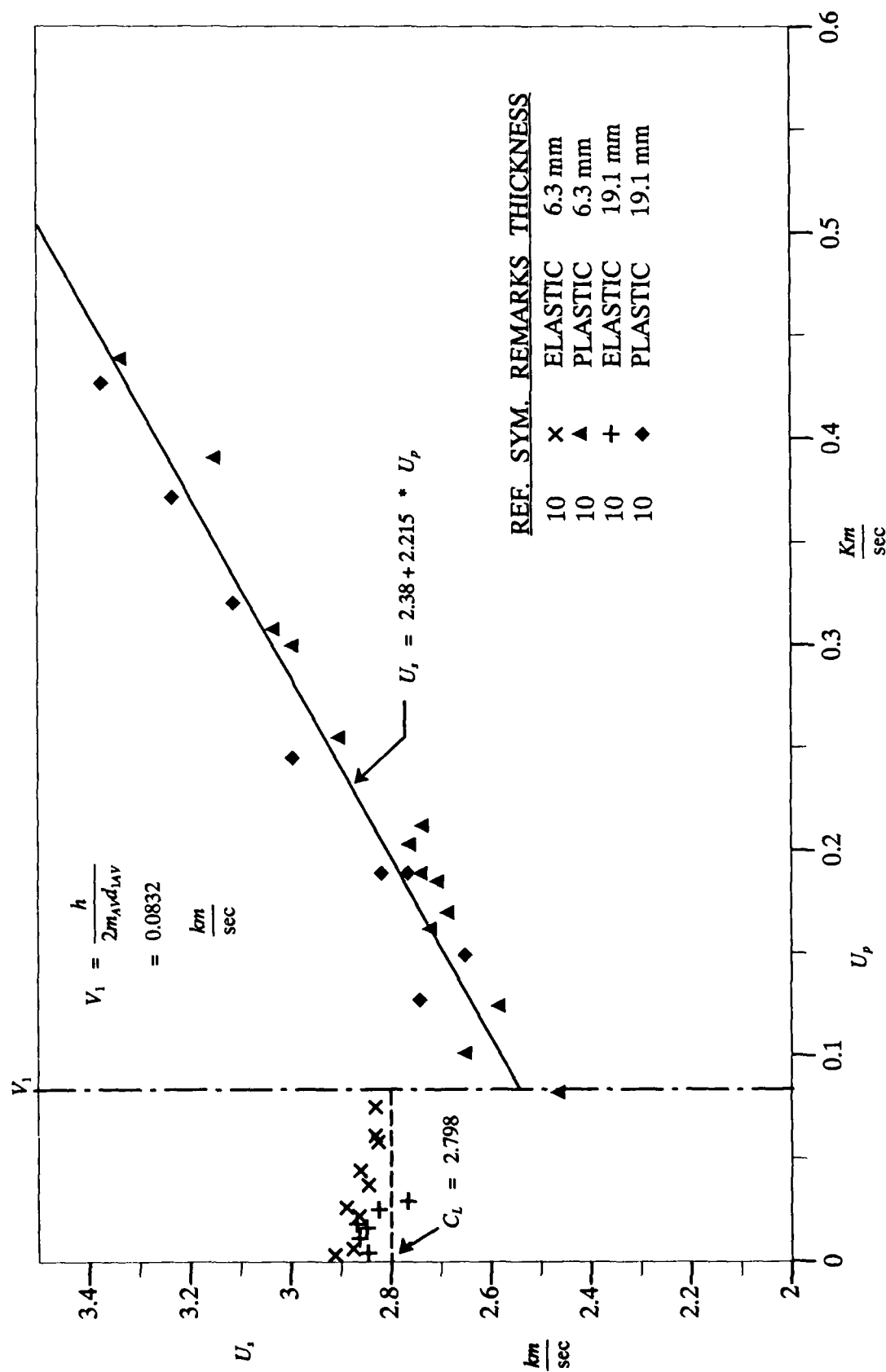


Figure 6. Elastic and Plastic Wave Front Velocity Versus Particle Velocity for Shocked TNT ($\rho_0 = 1.648\text{g/cc}$).

V. CONCLUSIONS

Although this is not an exhaustive investigation, enough information has been presented to indicate that:

A. A basic reason for EPSP to occur is because the De Broglie relation Eq. (1) specifies the limiting velocity (V_1) at which an atom of mass, m , can travel in an undistorted or stationary lattice structure where d_1 is the smallest distance between atoms. The plastic wave particle velocity is $U_p = h/(2md_1')$ so that the lattice spacing must change from d_1 to d_1' to accommodate the irresistibility driven particle. This is a rather violent and catastrophic event whose consequences are the same as a polymorphic phase change. A phase change causes a two-wave structure since the De Broglie relation must be satisfied by adjustments made to the atomic spacing in the new lattice structure. Thus there is one wave from the old lattice structure plus an additional wave from the new structure.

B. UpHEL for the stronger metals (iron 2024-T4 and 6061-T6) was generally between V_1 and $2V_1$. Apparently strong metallic atomic lattice bonding requires that UpHEL must be "overdriven" greater than V_1 to displace or distort the lattice plastically (reduce d_1 to d_1') and thus allow a plastic wave particle velocity which is $U_p = h/(2md_1')$.

C. The "weak" materials (annealed 2024 alloy and pressed TNT) did not require "overdriven" HEL particle velocities for formation of plastic waves. Essentially V_1 was an upper bound on HEL particle velocities for these materials.

D. V_1 is the steady state stable UpHEL for iron and 6061-T6, even when UpHEL had been overdriven as much as $2.4 V_1$. If sufficient time (or specimen thickness) was available, UpHEL decayed and asymptotically approached V_1 as a lower bound. This is consistent with Fitzgerald's [17] stability analysis for $V_1 < U_p < 2V_1$ which indicates that this is an unstable region.

E. Although UpHEL magnitudes may reach $2.4 V_1$ as shown for iron, most UpHEL values do not exceed $2V_1$. This is consistent with Fitzgerald's analysis showing the importance and criticality of $2V_1$.

IV. RECOMMENDATIONS

Additional EPSP data for other materials should be investigated for the De Broglie velocity, V_1 , influence at the HEL conditions. Certain anomalous behavior observed at low level shock loadings could possibly be explained as a V_1 effect. If this is suspected, then V_1 should be computed via Eq. (1) and compared with experimental particle velocities (U_p) in the region of interest.

REFERENCES

1. Minshall, Stanley, "Properties of Elastic and Plastic Waves Determined by Pin Contractors and Crystals." Journal of Applied Physics, Vol. 26, No. 4, pp. 463-469, April 1955.
2. Bancroft, Denison, Eric L. Peterson, and Stanley Minshall, "Polymorphism of Iron at High Pressures." Journal of Applied Physics, Vol. 27, No. 3, pp. 291-298, March 1956.
3. Hughes, D. S., L. E. Gourley, and Mary F. Gourley, "Shock Wave Compression of Iron and Bismuth." Journal of Applied Physics, Vol. 32, No. 4, pp. 624-629 April 1961.
4. Taylor, John W. and Melvin H. Rice, "Elastic Plastic Properties of Iron." Journal of Applied Physics, Vol. 34, No. 2, pp. 364-371, February 1963.
5. Barker, L. M., and R. E. Hollenbach, "Shock Study of the $\alpha \leftrightarrow \epsilon$ Phase Transition in Iron." Journal of Applied Physics, Vol. 45, No. 11, pp. 4872-4887, November 1974.
6. Barker, L. M., " α - Phase Hugoniot of Iron." Journal of Applied Physics, Vol. 46, No. 6, pp. 2544-2547, June 1975.
7. Fowles, G. R., "Shock Wave Compression of Hardened and Annealed 2024 Aluminum." Journal of Applied Physics, Vol. 32, No. 8, pp. 1475-1487, August 1961.
8. Lundergan, C. D. and Walter Herrman, "Equation of State of 6061-T6 Aluminum at Low Pressures." Journal of Applied Physics, Vol. 34, No. 7, pp. 2046-2052, July 1963.
9. Johnson, J. N. and L. M. Barker, "Dislocation Dynamics and Steady Plastic Wave Profiles in 6061-T6 Aluminum." Journal of Applied Physics, Vol. 40, No. 11, pp. 4321-4334, October 1969.
10. Wasley, R. J. and F. E. Walker, "Dynamic Compressive Behavior of a Strain - Rate Sensitive, Polycrystalline, Organic Solid." Journal of Applied Physics, Vol. 40, No. 6, pp. 2639-2648, May 1969.
11. Wasley, Richard J., Stress Wave Propagation in Solids; an Introduction, Marcel Dekker, Inc. New York, 1973.
12. Duvall, George E., "Some Properties and Applications of Shock Waves." Response of Metals to High Velocity Deformation, Proceedings of a Technical Conference, July 11-12, 1960, Editors P. G. Shewmon and V. F. Zackay, Interscience Publishers, Inc., pp. 165-203, New York, 1961.

13. Minshall, Stanley F., "The Dynamic Response of Iron and Iron Alloys to Shock Waves." Response of Metals to High Velocity Deformation, Proceedings of a Technical Conference, July 11-12, 1960, Editors P. G. Shewmon and V. F. Zackay, Interscience Publishers, Inc., New York, pp. 249-274, 1961.
14. McQueen, R. G., Marsh, S. P., Taylor, J. W., Fritz, J. N., and Carter, W. J., "The Equation of State of Solids From Shock Wave Studies." Hypervelocity Impact Phenomena, edited by Ray Kinslow, Academic Press, New York, pp. 293-417, 1970 .
15. Moore, Walter J., Physical Chemistry, Prentice - Hall Inc., Englewood Cliffs, N. J., 1962.
16. Daniels, Farrington, and Robert A. Alberty, Physical Chemistry, John Wiley and Sons, Inc., New York, 1966.
17. Fitzgerald, E. R., Particle Wave and Deformation of Crystalline Solids, Interscience Publishers, Inc., New York, 1966.
18. Billingsley, J. P. and C. L. Adams, Applications of Crystal Lattice Disintegration Criteria to Compute Minimum Shock Induced Reactive Conditions in Solid Explosive Materials, RD-SS-10, Aeroballistics Analysis Branch, Systems Simulation and Development Directorate, Research, Development, and Engineering Center, U. S. Army Missile Command, Redstone Arsenal, AL, March 1989.
19. Taylor, J. W., "Thunder in the Mountains.", Shock Waves in Condensed Matter 1983 , Elsevier Publishing Co., Inc., New York, 1984.
20. Taylor, J. W., "Dislocation Dynamics and Dynamic Yielding." Journal of Applied Physics, Vol. 36, No. 10, pp. 3146-3150, October 1965 .
21. Bell, J. F., The Physics of Large Deformation of Crystalline Solids, Springer-Verlag, New York, Inc., 1968.

DISTRIBUTION LIST

AMSMI-RD,	1 copy
AMSMI-RD-CS-R	15 copies
AMSMI-RD-CS-T	1 copy
AMSMI-GC-IP, Mr. Fred M. Bush	1 copy
 U.S. Army Material System Analysis Activity	 1 copy
ATTN: AMXSY-MP (Herbert Cohen)	
Aberdeen Proving Ground, MD 21005	
 IIT Research Institute	 3 copies
ATTN: GACIAC	
10 W. 35th Street	
Chicago, IL 60616	
 Sandia National Laboratories	 3 copies
ATTN: Dr. D. D. Bloomquist	
P. O. Box 5800	
Division 1252	
Albuquerque, NM 87185	
 Los Alamos National Laboratory	 3 copies
ATTN: Dr. Steven A. Sheffield	
Group M-9	
Mail Stop P-952	
Los Alamos, NM 87545	
 Antiarmor Munitions	 3 copies
Technical Office	
ATTN: AMCLO-AM, Dr. P. Howe	
Building 328	
Aberdeen Proving Ground, MD 21005-5006	
 Explosives Effects Branch	 3 copies
ATTN: SLCBR-TB-EE, Dr. R. Frey	
Aberdeen Proving Ground, MD 21005-5066	
 Los Alamos National Laboratory	 3 copies
ATTN: Dr. I. E. Lindstrom	
Group WX-5	
Mail Stop G-780	
Box 1663	
Los Alamos, NM 87545	

Naval Surface Weapons Center ATTN: R12, Mr. J. M. Short White Oak Silver Spring, MD 20903-5000	3 copies
Naval Surface Warfare Center ATTN: Mr. Tom Wasmund Code G-13 Dahlgren, VA 22448	3 copies
Eglin Air Force Base ATTN: AD/CZL, Mr. Bill Dyess Eglin, AFB, FL 32542-5000	3 copies
Mr. J. W. Watt 4068 Adams Drive Silver Spring, MD 20902	3 copies
Eglin Air Force Base ATTN: AD/ALJW, Dr. Joe Foster Eglin, AFB, FL 32542-5000	3 copies
TASC ATTN: Mr. Charles E. Clucus 907 Mar-Walt drive Fort Walton Beach, FL 32548	2 copies
University of Alabama at Huntsville (UAH) Research Institute ATTN: Mr. C. L. Adams Dr. B. Z. Jenkins Huntsville, AL 35816	5 copies 1 copy
Johns Hopkins University ATTN: Professor E. R. Fitzgerald 127 Latrobe Hall 34th and Charles Street Baltimore, MD 21218	10 copies
University of Illinois Department of Aeronautical Engineering ATTN: Professor R. A. Strehlow Urbana, IL 61801	3 copies
One Daniel Burnham Court ATTN: Dr. S. W. Yuan Apartment 1222 San Fransisco, CA 94109	2 copies

Los Alamos National Laboratory Dr. James P. Ritchie, Group Leader, Detonation Theory and Applications M. S. B214 Los Alamos, NM 87545	3 copies
Sandia National Laboratories Dr. Mark B. Boslough, Member Technical Staff Shock Wave and Explosives Physics Albuquerque, NM 87185	3 copies
Ms. Brigitta Dobratz 543 Todd Loop Los Alamos, NM 87544	2 copies
Dr. W. C. Davis, President Energetic Dynamics 693 4th Street Los Alamos, NM 87544	2 copies
Mr. James Dahn Safety Consulting Engineers, Inc. 5240 Pearl Street Rosemont, IL 60018	2 copies
Sandia National Laboratory ATTN: Dr. G. I. Kerley Division 1533 Albuquerque, NM 89185	3 copies
Lawrence Livermore National Laboratory ATTN: Dr. M. Van Thiel P. O. Box 808 Livermore, CA 94550	3 copies
Lawrence Livermore National Laboratory ATTN: Dr. Richard J. Wasley P. O. Box 808 Livermore, CA 94550	3 copies
Commander, U. S. ARDEC SMCAR-AEE-W(W) ATTN: Mr. B. Fishburn Picatinny Arsenal, NJ 07806-5000	3 copies
Commander, U. S. ARDEC SMCAR-CCH-V ATTN: Mr. Floyd Hildebrand Picatinny Arsenal, NJ 07806-5000	3 copies

Dr. Micheal R. Edwards Royal Military College of Science Department of Mechanical and Civil Engineering Shrivenham, Swindon, Wilts SN68LA, United Kingdom	1 copy
Office of Weapons Safety ATTN: Dr. Charles Karnes Science Advisor D.P. 22 U.S. Dept. of Energy Washington, D.C. 20545	3 copies
Sandia National Laboratory ATTN: Dr. R. A. Graham P.O. Box 5800 ORG, 1153 Albuquerque, NM 87185	3 copies
Denver Research Institute University of Denver ATTN: Mr. Larry Brown Denver, CO 80208	3 copies
Director, U.S. Army Ballistic Research Laboratory ATTN: Dr. John H. Suckling SLCBR-VL-V Aberdeen Proving Ground, MD 21005-5066	3 copies
Director, U.S. Army Ballistic Research Laboratory ATTN: Dr. T. N. Wright SLCBR-TB Aberdeen Proving Ground, MD 21005-5066	3 copies
Argonne National Laboratory, Technical Information Services Report Unit BLDG. 203 Argonne, IL 60439	3 copies
Department of Mechanical and Aerospace Engineering ATTN: Dr. Yukie Horie North Carolina State University Raleigh, NC 27695	2 copies
Department of Mathematics ATTN: Dr. Julian Wu North Carolina State University Raleigh, NC 27695	2 copies

Director, U.S. Army Research Office SLCRO-MS, Dr. Kailasam Iyer Dr. Michel Cistan P.O. Box 12211 Research Triangle Park, NC 27709-2211	2 copies
Los Alamos National Laboratory ATTN: Dr. J. J. Dick M-9 Mail Stop P952 Los Alamos, NM 87545	3 copies
Los Alamos National Laboratory ATTN: Dr. Jerry Wackerle Mail Stop P952 Los Alamos, NM 87545	3 copies
Department of Physics ATTN: Dr. G. E. Duvall Washington State University Pullman, WA 99164-2814	3 copies
ATTN: Dr. Y. M. Gupta Shock Dynamics Laboratory Dept. of Physics Washington State University Pullman, WA 99164-2814	3 copies
SFAE-AD-PA-JTMD, BG Capps	1 copy
SFAE-AD-PA-SE, Mr. Don Adams	1 copy
AMCPM-HA, COL Liberatore	1 copy
AMCPM-HA-SE-MS, Bernard Granger	1 copy
SFAE-AD-FM-TM, Mr. Jerry Brown	1 copy
AMSMI-RD-RE, Dr. J. S. Bennett	3 copies
AMSMI-RD-SS, Dr. Grider	1 copy
Mr. Davis	1 copy
AMSMI-RD-SS-SE, Mr. Grabney	1 copy
Mr. Jordan	1 copy
Mr. Waddle	1 copy
AMSMI-RD-SS-AA, Dr. Billingsley	10 copies
Mr. Head	1 copy
Dr. Oliver	5 copies
Mr. Ward	2 copies
AMSMI-RD-ST-CM, Mr. Parker	1 copy
Mr. Howard	1 copy
AMSMI-RD-ST-WF, Mr. Schexnayder	1 copy
Mr. Lovelace	1 copy
Mr. Lienau	1 copy
Mr. Hill	1 copy

Mr. Cornelius
Mr. MacDonald
AMSMI-RD-PR
AMSMI-RD-DE, Dr. Miles Holloman

1 copy
1 copy
3 copies
2 copies